Journal of Network Intelligence
Taiwan Ubiquitous Information
 ISSN 2414-8105 (Online)
Volume **7**, Number **1**, February **2022**

Diagnosis Method of Power Transformer Winding Position Deviation based on Frequency Response Analysis

Xi Song

State Grid Gansu Electric Power Supply Company
Lanzhou City, Gansu Province, 730030, China

Hehui Zhang

State Grid Gansu Electric Power Research Institute
Lanzhou City, Gansu Province, 730070, China

Wenhui Li

State Grid Gansu Electric Power Supply Company
Lanzhou City, Gansu Province, 730030, China

Jixiang Liu

State Grid Gansu Electric Power Research Institute
Lanzhou City, Gansu Province, 730070, China

Renping Song

Gansu Tongxing Intelligent Technology Development Co., Ltd.
Lanzhou City, Gansu Province, 730000, China

Bo Wang

kitami institute of technology,Department of Computer Science
65 koen-cho kitami, hokkaido 090-8507,Japan

Qiang Yin*

Northeast Electric Power University
No.169 Changchun Road, Jilin City, Jilin Province, 132012, China
*Corresponding Author: yinq980213@163.com

Received: July 2021; Revised: September 2021

Abstract. *The fault probability of power transformer is an important parameter in power modification planning. One of the main causes of power transformers failure is the breakage of insulators (such as insulating paper and gaskets) due to the electromagnetic force generated by high short-circuit current. The axial-displacement of winding may cause the increase of electromagnetic force; Thus, it is essential to diagnose it quantitatively. We had proposed a fault probability analysis method of the winding axial-displacement (AD) due to the increase of electromagnetic force. In this method, frequency response analysis is used to diagnose AD quantitatively. In the proposed method, it is necessary to obtain the existing measurement data in advance, which almost does not exist in practice. In the diagnosis of AD of winding in FRA, this paper presents a hierarchical analysis method of failure probability of power transformers considering the absence of measured reference data. One of the key techniques of graded evaluation is to diagnose AD without measured reference data. In view of the bipolar characteristics of resonance in the measured transfer function of inductive inter-winding, the FRA method of AD diagnosis without measuring reference data is proposed in this paper.*
Keywords: Power transformers failure; Frequency response analysis; AD diagnosis

1. **Introduction.** Power transformer is one of the important equipment of power system whose normal operation is directly related to the safety of power system. The winding short-circuit strength and structural stability in power transformers is always one of the main aspects of power transformer fault research [1,2]. In the process of transformer operation, the huge system short circuit current is the main cause of transformer winding deformation, especially in the transformer outlet or near the short circuit fault where is more serious. At present, winding deformation is still one of the main causes of transformer failure directly or indirectly [3].

Among the structural abnormalities of windings, the axial position deviation is the most dangerous. When the external short-circuit accident occurs in the misaligned state of the winding, the larger short-circuit current flows into the transformer winding, which may produce larger axial electromagnetic mechanical force than the design value. Due to this large axial electromagnetic mechanical force, insulating materials such as insulating paper and spacers are damaged, which may lead to internal short-circuit faults and grounding faults. Focusing on the possibility that the electromagnetic mechanical force and the resulting transformer failure probability (PB failure probability) increase due to the position deviation of winding axis, this paper proposes a transformer failure probability evaluation method when the winding deviates from the axial position.

Among them, the diagnosis of deterioration related to insulation strength and the diagnosis of axial position deviation of winding related to the increase of electromagnetic mechanical force are important elements. Insulation deterioration diagnosis can be applied based on transformer load history. On the other hand, with regard to the diagnosis of the amount of axial position deviation of the windings, recent studies have been carried out on small die transformers using the winding deviation position. Among them, Frequency Response Analysis (FRA) is applied to small modal transformers. In the transfer function measurement category specified in the international standard IEC 60076-18:2012, the transfer function of inter-winding conductivity measurement is proved to be sensitive to winding position deviation. In addition, a circuit model is proposed to reproduce the transfer function, and a quantitative diagnosis method for winding position separation using the circuit model is proposed.In essence, FRA method is used to detect transformer winding deformation, which is based on the mechanism that the frequency response characteristics of transformer windings change when the parameters of unit length inductance, longitudinal capacitance and capacitance to ground change after winding deformation [4,5]. When FRA measurement is carried out on an actual power transformer, there are only a limited number of testable terminals, especially before the cap [6]. The test process of frequency response analysis is as follows: The sinusoidal sweep signal is injected into a port of the winding $U_i(n)$, and the input and output voltage signals $U_o(n)$ and $U_i(n)$ corresponding to the sampling frequency are detected and received according to the signal acquisition information instrument. According to the frequency response function, the voltage ratio transfer function $H(n)$ of the coil model of the power transformer and the frequency response characteristic curve of the winding are obtained. Therefore, once the transformer winding or wire cake appears displacement or deformation, it will cause the relevant equivalent inductance L and capacitance parameter C to be different, and eventually cause the deviation of frequency response characteristic curve or the change of amplitude [7].

2. **Related Work.** The axial position deviation of transformer winding is one of the most dangerous structural anomalies among the abnormal structure of winding [8]. If the

external short circuit accident occurs under the condition of the misalignment of the winding, the larger short circuit current flows into the transformer winding, which is possible to produce greater axial electromagnetic mechanical force than the design value. Because of this large axial electromagnetic mechanical force, it is possible to damage insulating materials including insulating paper and gaskets, leading to internal short circuit fault and ground fault [9,10].

At present, transformer winding deformation testing is mainly based on two principles of three different testing methods, one is spectrum analysis principle, the other is short-circuit impedance testing principle. The principle of spectrum analysis includes sweep frequency test method (often called frequency response method) and low-voltage pulse test method. The principle of short-circuit impedance test is to test the transformer's low-voltage short-circuit impedance. Among the above three methods, the low-voltage pulse method has high sensitivity, but poor anti-electromagnetic interference ability and unstable pulse signal source. Due to the limitation of precision and repeatability of field testing instrument, the error rate of short-circuit impedance analysis is high. Frequency response analysis method (FRA) can reflect and diagnose winding deformation fault sensitively, and it is easy to use in the field, and can detect winding deformation without hanging cover. Compared with impedance method, frequency response spectrum contains more information about winding characteristics and is more sensitive to winding deformation.

Frequency response analysis method can be used to detect whether the transformer winding has global or local deformation, determine the deformation phase, and infer the degree and position of deformation. For traction transformer, the variation of frequency response curve before and after winding failure can reflect the deformation degree of winding to a certain extent. A large number of tests and field measurements show that it can be used to judge whether the winding has local deformation such as short circuit between turns or between cakes, distortion and bulges, as well as the whole winding displacement or the lead displacement.

Based on the electromagnetic mechanical force generated and the possibility that the fault probability will increase due to the offset of the spools [11], this paper presents a fault probability analysis method when the position of the spools is offset. Among them, the key technologies are the diagnosis of deterioration related to the strength of insulation and the diagnosis of the position offset around the spool related to the increase of electromagnetic mechanical force. A method has been designed for diagnosing insulation deterioration based on transformer load history. On the other hand, with regard to the diagnosis of the axial position offset of the winding, the research of the small winding transformer using the position offset of the winding has been carried out recently [12]. Among them, FRA is applied in small core transformer, and the high sensitivity of transfer function to the deviation of winding position is studied. In addition, a circuit model to reproduce the transfer function is proposed, and the possibility of using the circuit model to diagnose the position deviation of the winding is discussed [13]. This paper will describe the diagnosis method of transformer winding position deviation with detailed data. In addition, the transformer fault probability analysis method using the method of wound position deviation is introduced [14].

3. **Probability analysis of power transformer failure based on FRA.**

3.1. **Probability analysis method of transformer failure and its component technology.**

Under the condition of position deviation of transformer winding, the flow of the transformer failure probability analysis method is proposed in this paper as shown

in Figure 1. Firstly, the process calculates the electromagnetic mechanical force generated inside the transformer when an external short circuit occurs in the state of the winding position deviation according to the diagnosis result of the winding position deviation. Then, according to the insulator degradation diagnosis performed, the mechanical strength of the insulator is estimated, and it is determined whether the insulator can resist electromagnetic mechanical force. At this time, the positional deviation of the winding and the deterioration state of the insulator are essential parameters, but since these are all obtained through diagnosis, there is uncertainty in the estimated value. Therefore, it is not a definite analysis of whether there is a failure, but an analysis of the probability of failure.

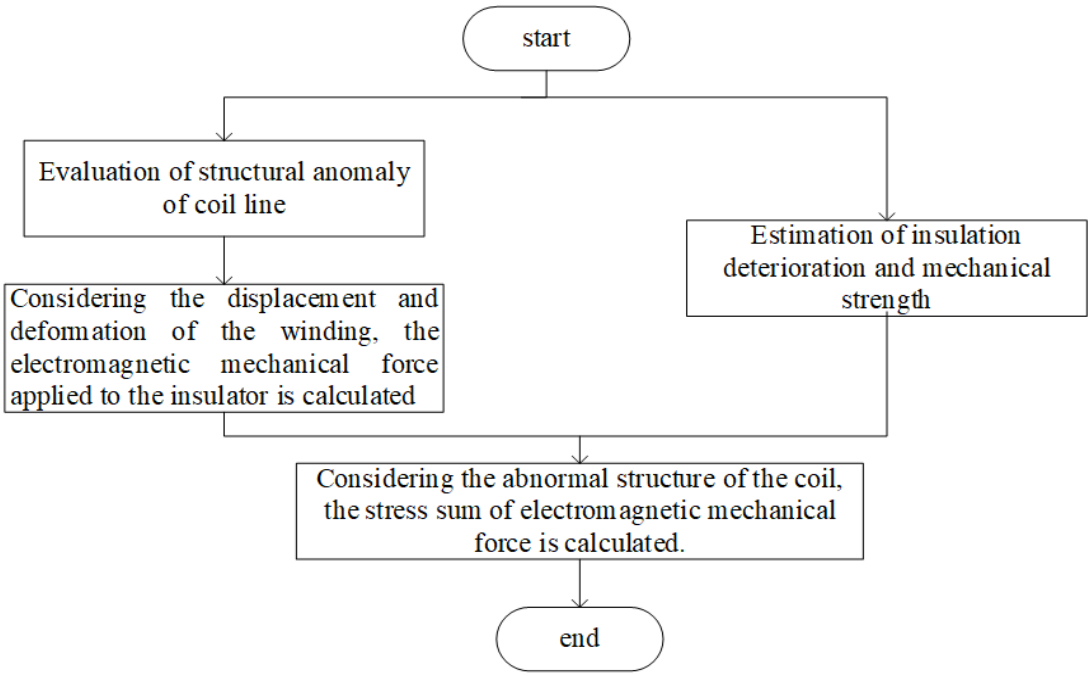

FIGURE 1. Flow chart of fault probability assessment considering abnormal winding structure of transformer

In the transformer failure probability analysis process above, key technologies are the winding position deviation diagnosis and winding deterioration diagnosis. As the winding deterioration diagnosis, a method of calculating the winding temperature history based on the transformer load history and estimating the deterioration state (average degree of polymerization of insulating paper) has been proposed which has been put into practical application. On the other hand, in terms of winding position deviation diagnosis, FRA connects a voltage source to a certain terminal of the transformer winding, and measures the voltage ratio and phase difference with other terminals in a wider frequency band. The measurement of the frequency response usually adopts the method shown in Figure 2, and the transfer function shown in Equation (1) is measured in the frequency range of several 10Hz several MHz.

$$\dot{T}F(\omega) = 20log\frac{V_o(\omega)}{V_i(\omega)} \tag{1}$$

Here, ω is the angular frequency. The transfer function of the transformer is determined by electrical parameters such as winding self-inductance, mutual inductance

between windings, phase-to-phase electrostatic capacitance, and ground electrostatic capacitance.

About FRA, when a structural abnormality such as transfer function measurement offset or seat flexion occurs, both the electrical parameters and the transfer function change. FRA compares the measured transfer function with reference data, and detects winding abnormalities based on whether there is a difference. As reference data, it is based on the transfer function measured in advance when the transformer is healthy.

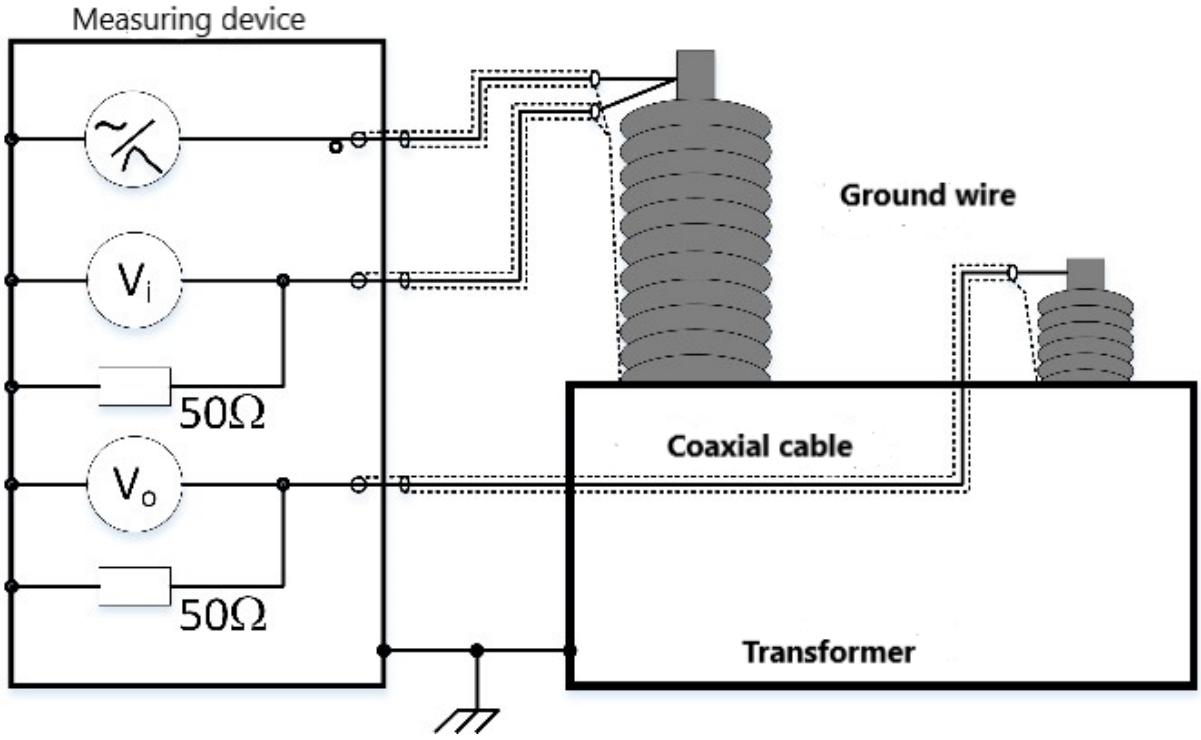

FIGURE 2. Transfer function measurement in FRA

3.2. **Measurement method of power transformer.**

3.2.1. *Power transformer.* The power transformer is shown in Figure 3, and its main specifications are shown in Table 1. The power transformer is a three-phase winding transformer with rated capacity of 160kva and rated voltage of 10.5kV/0.4kV. For simplicity, the three-phase winding is cut off and measured as a single-phase transformer. In addition, the wiring of YNyn0, YNd1, Yd1 and Dd03 is also measured.

Rubber insulation is inserted into the lower part of the winding of the power transformer. Four stamped plates with a thickness of 2mm are inserted between the V-phase high-voltage axis and the rubber insulator. Through moving one or two of them, the high-voltage axis deviates downward by 2mm or 4mm. The total height of high-voltage axis including insulation material is 450mm, so the axial position offset is equivalent to 0.44% and 0.89% of this value respectively. Previous studies on diagnosing the position deviation of transformer winding axis by FRA are all experimental studies aiming at the large amount of winding position deviation.

FIGURE 3. Research object transformer

TABLE 1. The main specifications of the transformer are discussed

Rated voltage	10.5kV/0.4kV
Rated capacity	160kV A
Connection and phase shift (vector group symbol)	·Single-phase YNyn0 Yy0 YNd1 Yd1 Dd0
High voltage winding height	450mm (including insulating material)
The reference appendix	· Mode transformer · Tap terminals outside the winding

In the normal state (refer to the state obtained by the data), the news board is inserted with 4 sheets, and 2 sheets are cut out of 4 mm position deviation, and the bottom of the news board is also wound state. A wooden spacer is inserted between the high-pressure axis and the low-pressure axis to prevent the winding from shifting in the horizontal direction.

3.3. **Evaluation of the sensitivity of the transfer function to the measurement result and the deviation of the winding position.**

3.3.1. *Measurement results.* As an example of the transfer function measurement result, Figure 4 shows the transfer function measured in the state of a single-phase transformer except for the connection of the transformer to be measured. It can be confirmed by visual inspection that due to the deviation of the winding position, the transfer function measured by the only IIW has changed around 50kHz Figure 4(h). Hereafter, from the point of view of its shape, this resonance is called bipolar resonance. In addition, when the one end of the winding is grounded in IIW measurement, the reproducibility of the measurement is greatly affected in the frequency band of hundreds of kHz or more, so be careful. In the transfer function of other measurement categories, no change due to the deviation of the winding position was found. Therefore, even if the three transfer functions are superimposed and plotted, it seems that only one transfer function is displayed.

TABLE 2. Numerical index of transfer function calculation for normal transformer and transformer with abnormal winding

Transfer function	$CCF^{1)}$	$CC^{1)}$	$SD^{2)}$	$SDA^{2)}$	$LCCF^{1)}$
Normal transformer	0.995	1.000	0.068	0.025	-2.64
Transformer with abnormal winding	0.991	0.999	0.113	0.023	-6.23

Based on the research using the transformer winding model, not only the IIW measurement, the transfer function of the CIW measurement also has a high sensitivity to the winding position deviation. However, in Figure 4(e), the transfer function measured by CIW hardly changes due to the deviation of the winding position. Maybe it is because the high-voltage and low-voltage winding interval in the transformer winding model is very narrow. In the transformer winding model, the ratio of the outer radius of the low voltage winding to the inner radius of the high voltage winding (winding diameter ratio) is 98%, while the ratio of the power transformer in this paper is 83%. When the winding diameter ratio is large, the electrostatic capacity between the high-voltage and low-voltage lines becomes larger, and it takes a dominant position in the transfer function measured by CIW. When the winding position deviation occurs, the electrostatic capacitance between high voltage and low winding will change. Therefore, the transformer winding model has a greater change in the transfer function when the winding diameter is relatively large. However, the winding diameter ratio of the transformer winding model is 98%, which is unrealistic to consider the insulation and cooling between windings.

3.3.2. *Evaluation of numerical indicators for detecting deviation of winding position.* In order to select numerical indicators useful for objectively determining whether there is a deviation in the winding position, various numerical indicators are calculated. In addition, CCF* is not displayed in Figure 4(a) , Figure 4(b), Figure 4(c), Figure 4(e), and Figure 4(f) because the transfer function has not changed and CCF*$\approx$ 0, which overlaps the upper frame of the graph. Here, the CCF* calculated in the frequency band below 1kHz in Figure 4(d) and below 10kHz in Figure 4(g) is a low value, but this does not mean that the transfer function is mismatched as described below. The transfer functions of these frequency bands are almost constant. Therefore, the comparison of transfer functions in this frequency band is equivalent to comparing overlapping noises, and CCF* represents a lower value. Therefore, this frequency band was excluded from the LCCF* analysis.

4. **Reproduce the transfer function through the circuit model.**

4.1. **Design scheme.** According to the experimental results in Section 3, the sensitivity of the transfer function measured by IIW is the highest, and the amplitude of bipolar resonance changes due to the position deviation in the bobbin direction. In this paper, a circuit model which can reproduce bipolar resonance with transfer function near 50kHz measured by IIW is proposed.

Figure 5 shows the proposed circuit model (1 phase). In Figure 5, the right side is the high-pressure axis and the left side is the low-pressure axis. Second additional word H or L of each symbol means high voltage and low voltage lines respectively. Excitation inductance Le, excitation Resistance Re and winding resistance Rw are adopted for each winding, and T-shaped circuit is adopted for modeling. In addition, the electrostatic capacitance of high voltage axis to ground, the electrostatic capacitance between high-voltage and low-voltage axis, the magnetic coupling coefficient of each inductor are also considered.

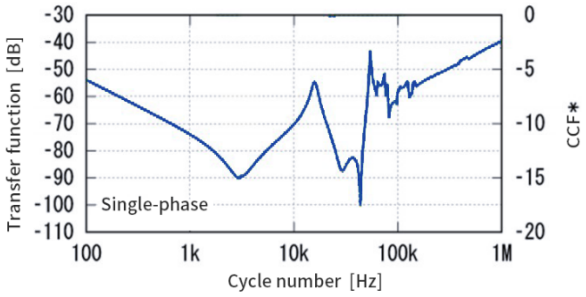

(a) OC determination (high voltage winding)

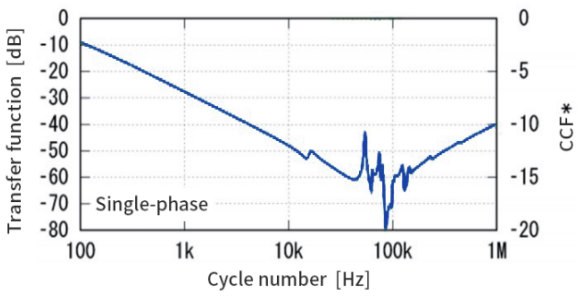

(b) SC determination(high voltage winding)

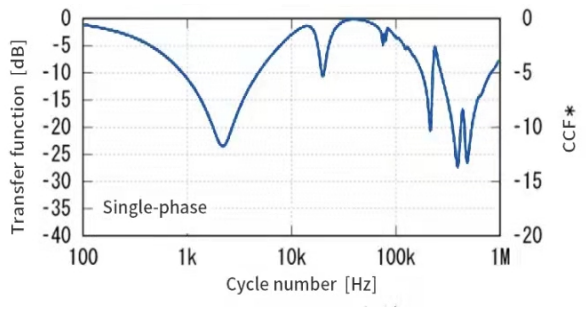

(c) OC determination (low voltage winding)

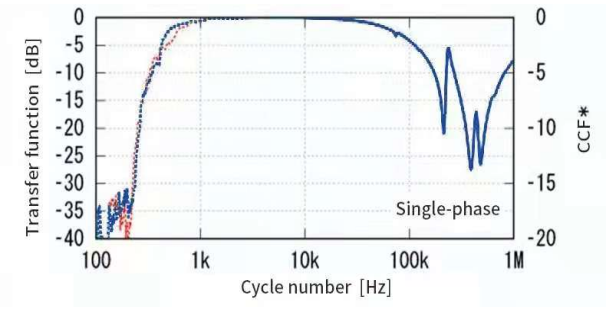

(d) SC determination (low voltage winding)

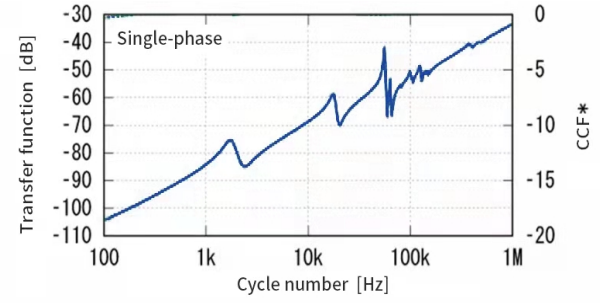

(e) CIW determination

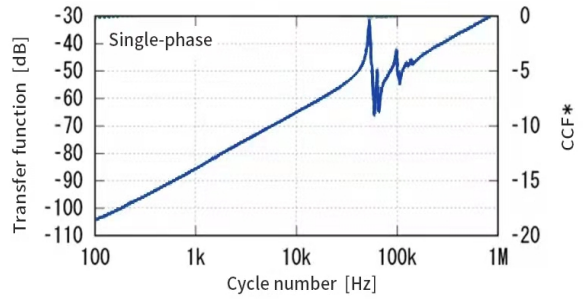

(f) CIW-SC determination

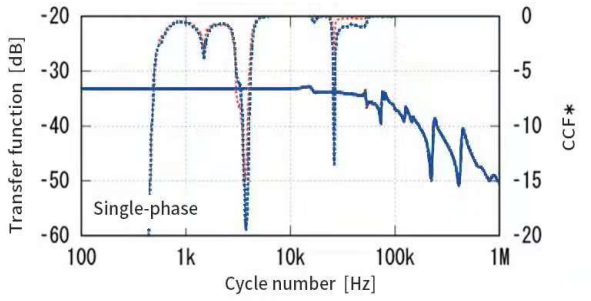

(g) IIW determination(100Hz-1MHz)

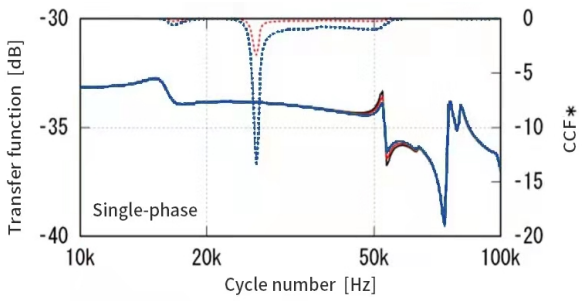

(h) IIW determination(10Hz-100Hz)

Transfer function(0mm)—— Transfer function(-2mm)——
Transfer function(-4mm)——CCF*(-2mm)– – – CCF*(-4mm)– – –

FIGURE 4. Measurement results of transfer function (in the case of single phase without connecting three-phase winding)

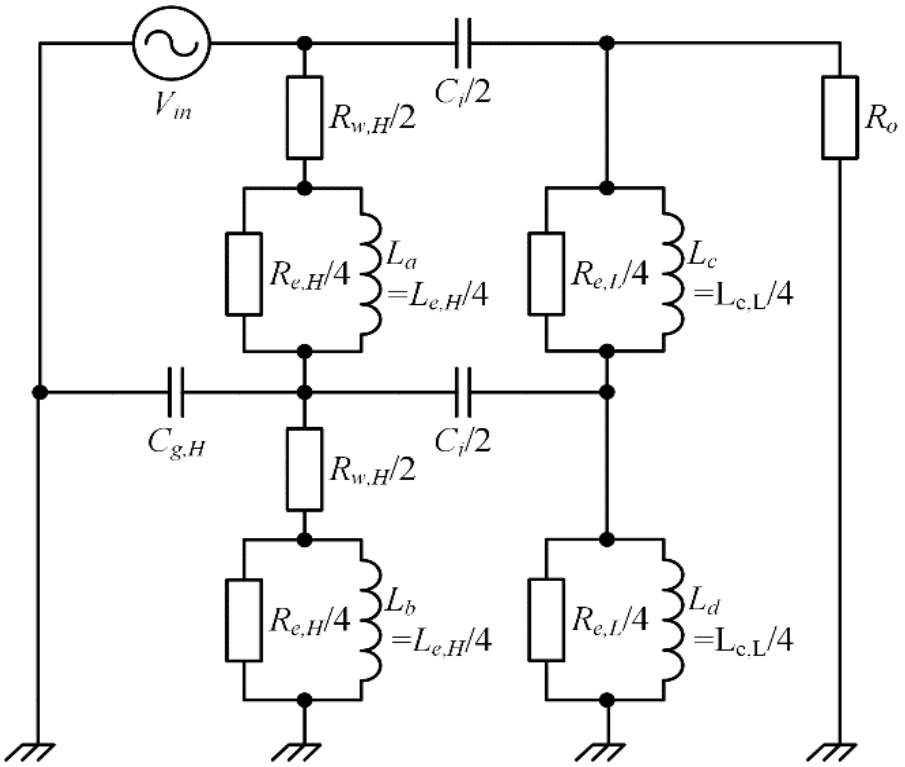

FIGURE 5. A circuit model is proposed to reproduce the bipolar resonance of the transfer function measured by IIW

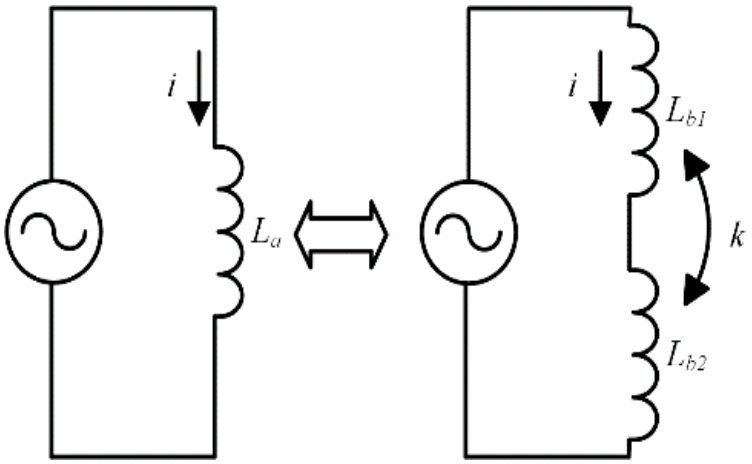

FIGURE 6. Inductance partition in circuit model

4.2. **The method of determining the parameters of the proposed model.** The parameters of the circuit model are determined according to the measurement results of the transfer function. This will be described in detail below.

(1) Magnetizing inductance viewed from the high-voltage side: $L_{e,H}$

In the transfer function measurement, the relationship between the impedance $Z(\omega)$ between the voltage input terminal and the output terminal and the transfer function

TF(ω) can be expressed by Formula (2).

$$\dot{T}F(\omega) = 20log\frac{50}{50 + Z(\omega)} \tag{2}$$

In the transfer function of the OC measurement of the high-voltage axis, in the frequency below the resonance of the lowest frequency, the impedance can be regarded as the impedance of the parallel circuit of the excitation inductance and the excitation resistance. Therefore, the magnetizing inductances $L_{e,H}$ seen from the high-voltage side can be determined based on the value of the transfer function of the frequency band. In the actual parameter determination, had better use low-frequency transfer function values as much as possible, which is to reduce the influence of the excitation resistance. For the following reasons, the proposed model uses 1/4 of the determined magnetizing inductance value as a parameter. In the proposed model, as shown in Figure 6, each winding is represented by a T-shaped model, and the magnetic coupling of two inductors is also considered. In Figure 6, the inductance *La* and the current flowing through L_{b1} and L_{b2} must be equal. This means that the total inductance is equivalent. According to this condition, Formula (3) holds.

$$\dot{L}_a\frac{d_i}{d_t} = L_{b1}\frac{d_i}{d_t} + L_{b2}\frac{d_i}{d_t} + 2k\sqrt{L_{b1}L_{b2}}\frac{d_i}{d_t} \tag{3}$$

Here, $k = 1$ and $L_{b1} = L_{b2}$, *formula (3)* can be written as Formula (4).

$$\dot{L}_a\frac{d_i}{d_t} = 4L_{b1}\frac{d_i}{d_t} \tag{4}$$

Therefore, in the proposed model, a value of 1/4 is adopted so that the total inductance is equivalent to the value determined from the measured value of the transfer function.

(2) Excitation inductance from low voltage side: $L_{e,L}$

The magnetizing inductance seen from the low-voltage side can be obtained by *equation* (5) using the magnetizing inductances $L_{e,H}$ seen from the high-voltage side and the winding ratio *a*.

$$\dot{L}_{e,L} = \frac{L_{e,H}}{a^2} \tag{5}$$

(3) Winding resistance of high voltage winding: $R_{w,H}$

In the transmission function of the high-quality part of the measurement line SC, in the resonance frequency below the lowest frequency (the example in Figure 4(b) is about 10khz or less), the impedance between measuring terminals can be considered as the impedance of the in-line circuit with high winding resistance and leakage inductance. Therefore, the winding resistances $R_{w,H}$ of the high-voltage axis can be determined by equation (2) using the transfer function value of this frequency band, and the leakage inductance can also be determined by the transfer function. At this time, the value of the transfer function uses the value of the frequency band in which the slope of the transfer function is constant. This is because the slope of the transfer function is within a certain frequency range, and the leakage inductance is dominant. At lower frequencies, the influence of winding resistance cannot be ignored. While at high frequencies, the influence of electrostatic capacitance cannot be ignored, resulting in inconstant tilt.

(4) The electrostatic capacity between high-voltage and low-voltage windings: C_i

In the transfer function measured by CIW-SC, when the slope of the transfer function is in a certain frequency band (about 20khz or less in the example of Figure 4(f)), the impedance between the measurement terminals can be regarded as a high-voltage-low-voltage line Impedance caused by the electrostatic capacitance between them. Therefore, the electrostatic capacitance Ci between the high-voltage and low-voltage lines can be determined by equation (2) using the transfer function value of this frequency band. In the actual parameter determination, had better use high-frequency transfer function values as much as possible. The higher the transfer function value, the higher the frequency, which means the greater the measured voltage at the output. Therefore, the higher the frequency, the smaller the influence of noise during measurement, and the parameters can be determined with high accuracy. This is the purpose of introducing CIW-SC measurement. In the transfer function measured by CIW-SC, the resonance of the lowest frequency occurs at a higher frequency than the transfer function measured by CIW. It can be seen that the frequency band with a constant slope of the above transfer function is wider. This is because the high-voltage and low-voltage lines are short-circuited respectively, so the inductance of the winding is not the magnetizing inductance, but the leakage inductance that is much smaller than the magnetizing inductance. Since the frequency band of the constant slope of the transfer function measured by CIW-SC is wider, CIW can more accurately determine the electrostatic capacitance between the high-voltage and low-voltage lines when the measurement is adopted.

(5) Magnetic coupling coefficient: k

The magnetic coupling coefficient k can be determined by Equation (6).

$$\dot{k} = \sqrt{1 - \frac{L_{l,H}}{L_{e,H}}} \tag{6}$$

Among them, $L_{1,H}$ are the leakage inductance of the high-pressure axis, as described in item (2), can be determined from the transfer function value measured by the SC of the high-pressure axis.

Among them, the proposed model uses 4 inductors per phase. Therefore, these combinations are $4C2 = 6$, and 6 magnetic coupling coefficients need to be determined. In the proposed model, the six magnetic coupling coefficients are basically the same. However, it is proposed to change the result of the calculation of the magnetic field coupling coefficient of the transfer function model. The magnetic field coupling coefficient between the high-quality part line and the low-quality part line inductance will affect the resonant resonance frequency of the reproduction object. Figure 4 (h) Broken line yen Part of the impact of the amplitude. Therefore, the magnetic field coupling coefficient $k1$(6) between the inductance of the high-quality part line and the inductance of the low-key part line is calculated by the Formula $k1$(6), and the magnetic field coupling coefficient $k2$ between the high-level part line and the low-level part line inductance is based on the value, the calculation result shows that the measured result is consistent with the decision.

(6) The electrostatic capacitance to ground of the high voltage winding: $C_{g,H}$

In the IIW measurement, one end of each winding is grounded. The electrostatic capacitance to ground in this state is physically different from the electrostatic capacitance to ground of the winding measured in the factory test, which is difficult to measure. Therefore, by the following method, the calculated resonant frequency of the bipolar resonance of the transfer function is consistent with the measured result.

Through the calculation results of changing the parameters of the proposed model, it can be known that:

· The current $I_{Cg,H}$ of the electrostatic capacitance to ground flowing to the high-voltage axis has the same resonance frequency as the bipolar resonance of the current reproduction target.
·The resistance and inductance of the low-voltage line do not affect the resonance frequency.

On this basis, the circuit that ignores the resistance and inductance of the low-voltage line is studied. In this circuit, $I_{Cg,H}$ are written in Equation (7).

$$\dot{I}_{Cg,H} = \frac{j\omega C_{g,H}}{8 - (C_{g,H} + \frac{C_i}{2})(1-k)L_{e,H}\omega^2} \tag{7}$$

Set the denominator of Equation (8) to zero, and the resonance frequency is represented by Equation (8).

$$\dot{f}_r = \frac{\sqrt{2}}{\pi\sqrt{(C_{g,H} + \frac{C_i}{2})(1-k)L_{e,H}}} \tag{8}$$

Therefore, using the actual measured value *fr* of the resonance frequency, the mutual coupling coefficient k, the magnetizing inductance $L_{e,H}$ from the high-voltage side, and the electrostatic capacitance C_i, $C_{g,H}$ between the high-voltage and low-voltage windings can be calculated by Equation (9).

$$\dot{C}_{g,H} = \frac{2}{\pi^2(1-k)L_{e,H}f_r^2} - \frac{C_i}{2} \tag{9}$$

(7) Excitation resistance viewed from the high and low voltage side: $R_{e,H}$, $R_{e,L}$

The magnetizing resistance ($R_{e,H}$ and $R_{e,L}$) viewed from the high-voltage side and the low-voltage side can basically be determined in the same way as the magnetizing inductance shown in items (1) and (2). However, it is well known that the excitation resistance has a strong frequency dependence, and it is difficult to determine them from the value of a frequency transfer function. Therefore, the calculation results of these magnetizing inductances determine the transfer function are in good agreement with the measurement results. At this time, the ratio of the field resistance observed from the high-voltage side and the low-voltage side is constant ($R_{e,L}/R_{e,H}$=*a2*) of the square of the winding ratio. These excitation resistances mainly affect the amplitude of the bipolar resonance around 50khz, which is the object of reproduction.

4.3. **Reconstruction of the transfer function based on the proposed model.** Figures 7(a-I) (d-I) show the measurement results of the transfer function and the calculation results according to the proposed model in the state where there is no deviation of the winding position. The proposed model reproduces the bipolar resonance very well.

While keeping the total inductance of the high-voltage axis of Figure 5 unchanged, the winding position deviation is simulated by increasing or decreasing them. Figures 7 (a-II) to (d-II) and (a-III) to (d-III) show transfer functions calculated in this way. The calculation result of the transfer function reproduces the measured bipolar resonance of the transfer function well.

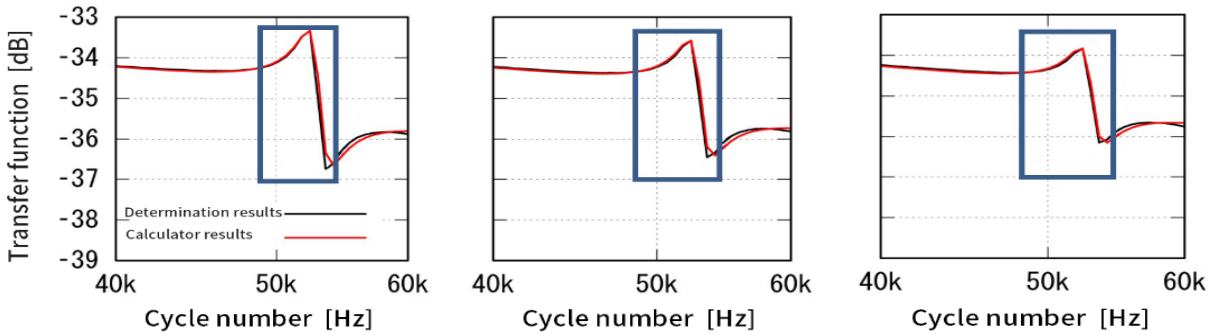

(a) 0mm(Coil height ratio: 0%) (b) -2mm(ratio: 0.44%) (c) -4mm(ratio: 0.89%)

(I) single-phase

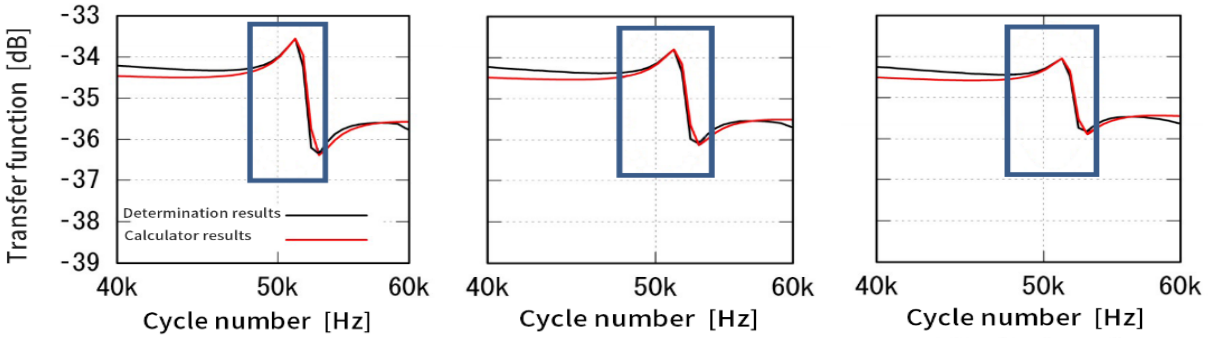

(e) 0mm (f) -2mm (g) -4mm

(II) YNyn0

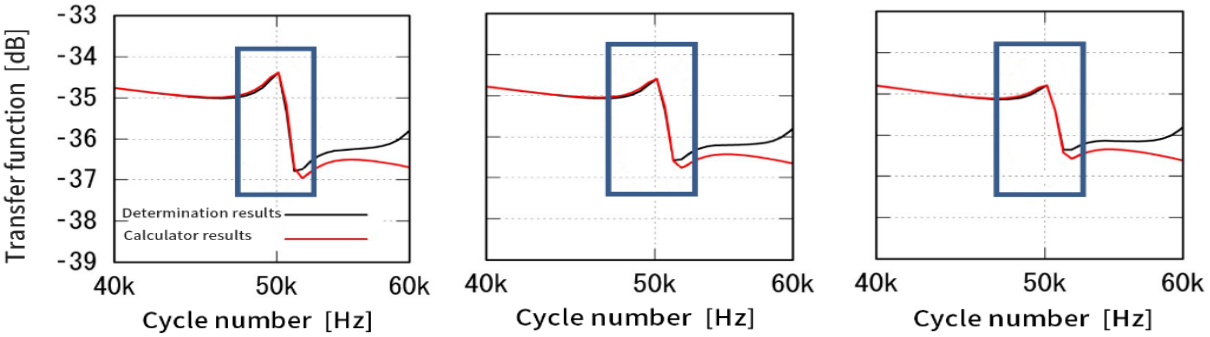

(i) 0mm (j) -2mm (k) -4mm

(III) Yy0

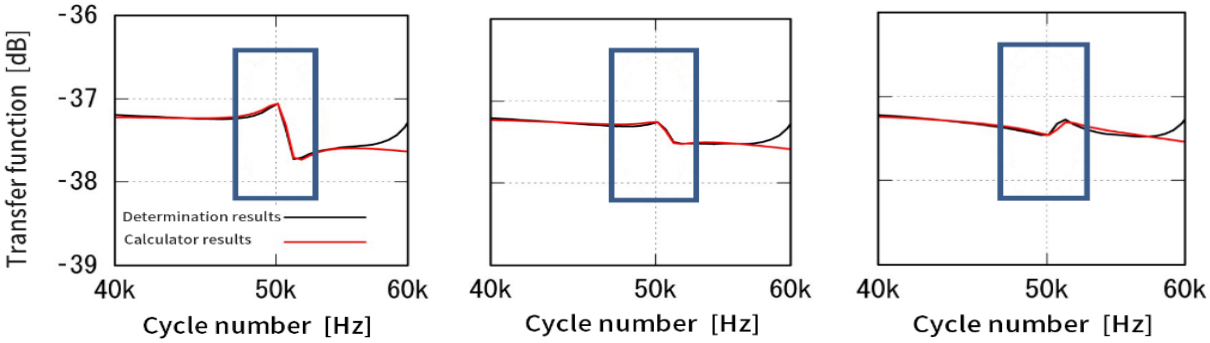

(m) 0mm (n) -2mm (o) -4mm

(IV) Yd1

FIGURE 7. Reconstruction results of transfer function based on proposal model)

Figure 8 shows the relationship between the increase/decrease rate of the high-voltage axis inductance and the winding position shift amount when the bipolar resonance is reproduced in Figure 7. Here, the upward direction of the winding position deviation is defined as positive, and the increase or decrease rate when the upward inductance of the circuit model increases is defined as positive. It can be seen that there is a linear relationship between the two. Based on this relationship, it is possible to perform a quantitative diagnosis of the winding position deviation through the following steps.

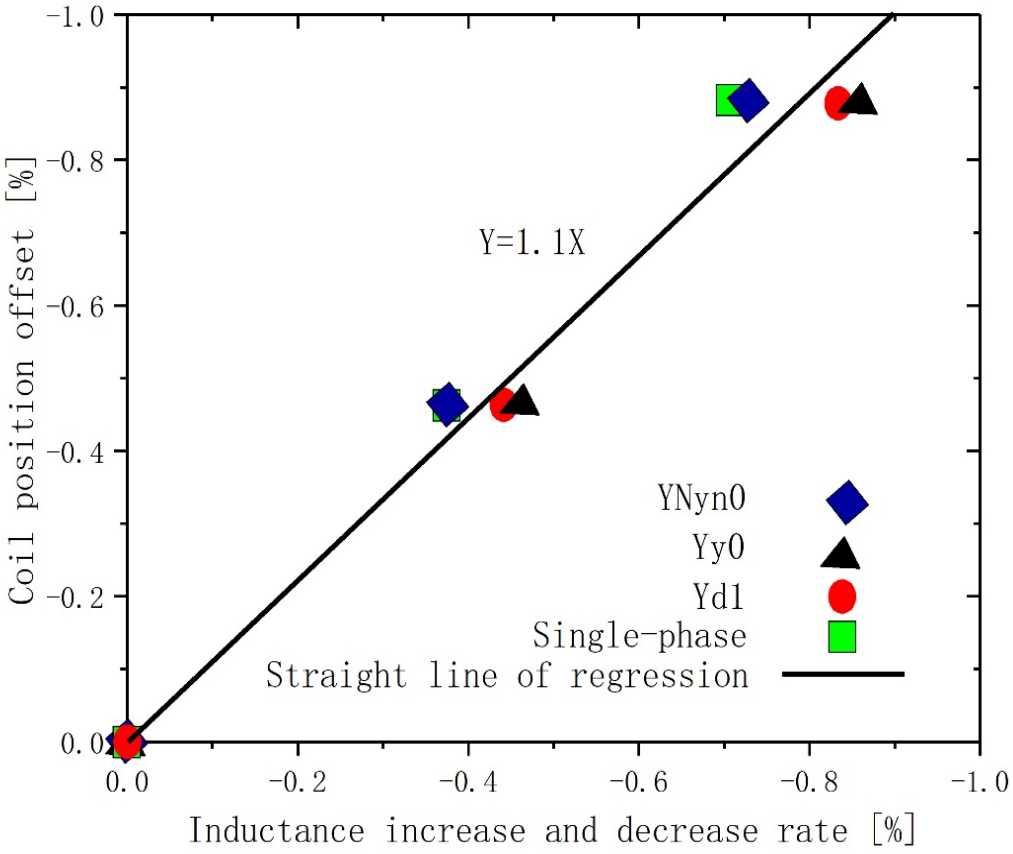

FIGURE 8. Reproduce the relationship between the increase / decrease rate of the measured inductance of bipolar resonance and the deviation of winding position

1) Using the proposed model, the bipolar resonance of the transfer function (historical data) measured by IIW under the normal state of the winding without misalignment is reproduced.
2) The bipolar resonance of the transfer function (diagnostic data) measured by the IIW measured at the time of diagnosis is reproduced by adding or subtracting the high-voltage axis inductance from the model that reproduces the past data in 1).
3) Based on the high-voltage axis inductance increase and decrease rate of the model of the reproduced diagnostic data of the bipolar resonance, the winding position deviation is estimated by the regression line (Figure 8). This scheme uses numerical indicators instead of winding positions.

5. **Discussion on the analysis method of transformer failure probability.** When the diagnosis result of transformer winding position deviation is applied to transformer failure probability analysis, the diagnosis accuracy is an essential factor. Here, the diagnosis result does not indicate the actual amount of misalignment with a certain value,

and it can be considered that the actual amount of misalignment is within a certain range centered on the diagnostic value. When diagnosing the winding position deviation of the actual transformer, it can be expected that the probability of the actual position deviation being close to the diagnosis value is high, and the probability of deviating from the diagnosis value is low. Therefore, the amount of misalignment can be expressed by a certain probability distribution centered on the diagnostic value. It is assumed that the probability distribution of the deviation of the winding position is represented by a normal distribution centered on the diagnostic value to analyze the probability of transformer failure. Also consider the probability distribution of the mechanical strength of the insulator. Here, it is considered that the calculation based on the load history is adopted for the mechanical strength diagnosis (deterioration diagnosis) of the insulator. This method is applied to the dismantling of the transformer, the average degree of polymerization of the insulating paper calculated manually is compared with the measured value, and the error obtained is expressed in the degree distribution, as shown in Figure 9. The average error is 0.1% and the standard deviation is 12.7%. The standard deviation can be used as the standard deviation of the estimated probability distribution of the average degree of polymerization of the insulating paper. On the other hand, in order to evaluate the standard deviation of the probability distribution of the winding position deviation (electromagnetic mechanical force generated during an external short circuit) estimated by the proposed method, it is necessary to update the regression line of Figure 7 according to the actual transformer data and accumulate the data. However, assume that the standard deviation calculated for the data in Figure 6 is 8.4%. Figure 10 shows the analysis result regarding the influence of the accuracy (standard deviation of the probability distribution) of the deterioration diagnosis and the winding position deviation diagnosis in the transformer failure probability analysis on the analysis result.

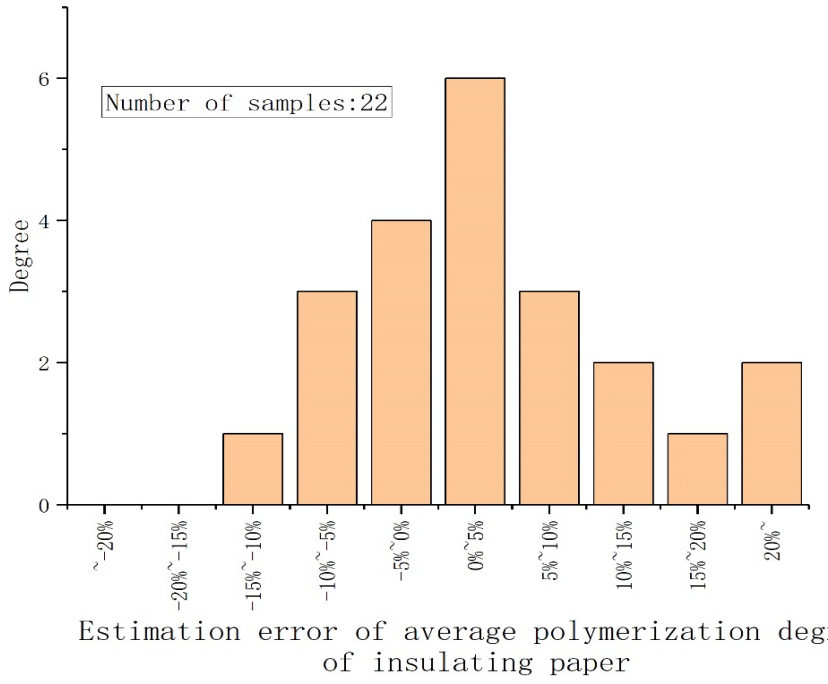

FIGURE 9. Error evaluation results of calculating average polymerization degree of insulation paper based on transformer load history

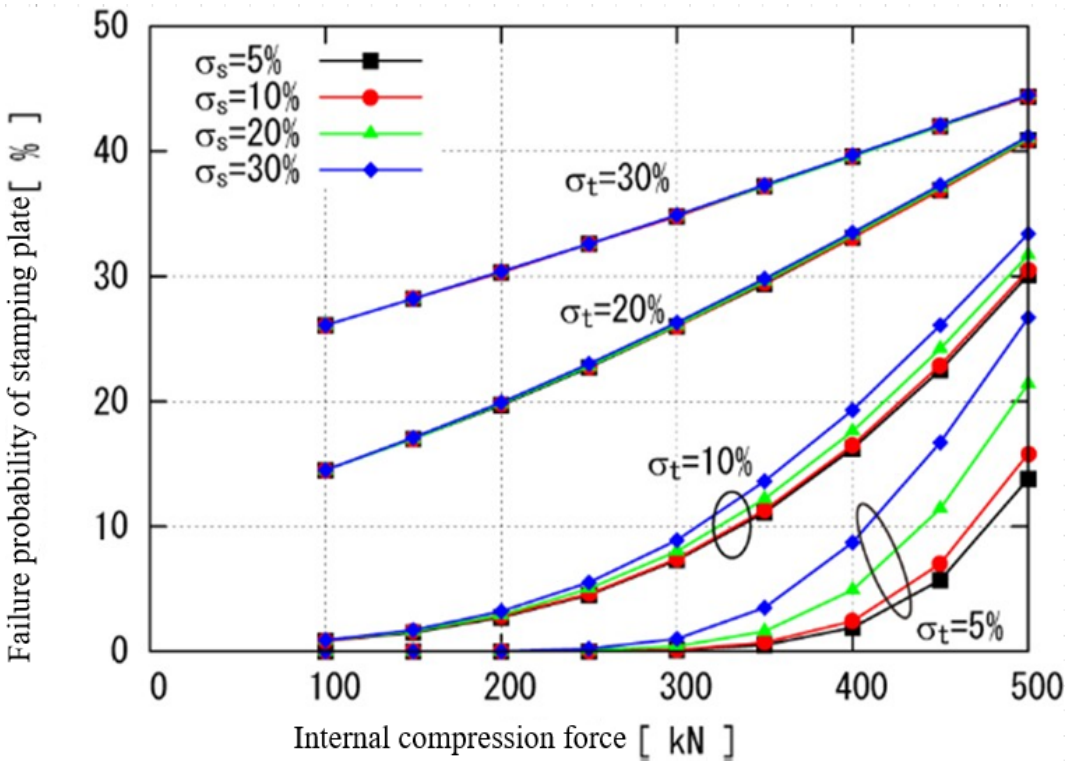

FIGURE 10. Evaluation of the influence of the accuracy of deterioration diagnosis and coil position deviation diagnosis on the results of transformer fault probability evaluation

As a deterioration diagnosis method based on the transformer load history method, the standard deviation of the probability distribution of the mechanical strength of the insulator $\sigma\ t = 12.7\ \%$, the standard deviation of the probability distribution of the compressive stress σs (the standard deviation of the probability distribution of the estimated value of the winding position deviation) As a hypothesis, $\sigma s = 8.4\%$ is evaluated. From the analysis result of the damage probability in Figure 10, it can be said that it hardly affects the smaller. Therefore, although detailed inspections must be carried out in the actual transformer verification in the future, the proposed method is a promising method in the diagnosis of the winding position deviation in the failure probability analysis when the transformer is externally short-circuited.

6. **Conclusions.** This article introduces a research example of diagnosis method of winding position deviation of power transformer based on FRA, which can be applied to the analysis of the transformer failure probability when an external short circuit occurs. Among them, through shifting the position of the high-voltage axis of the small modal transformer, the results of measuring the transfer functions of various measurement categories show that the IIW measurement has the highest sensitivity to the winding position shift. In particular, the change of the bipolar resonance is large. Among the numerical indicators to objectively detect the change through comparison with historical data, the LCCF* in the moving cross-correlation coefficient method is the most useful. In addition, the circuit model reproduces the bipolar resonance in the normal state and the winding position shift state, and finds the possibility of diagnosing the winding position shift amount. This scheme is based on the research results of small modal transformers, and

it must be verified with actual transformers in the future. However, this method is expected to be applied to the diagnosis of winding position deviation in transformer failure probability analysis when the transformer is externally short-circuited.

REFERENCES

[1] T. Sano, K. Miyagi, Experimental investigation on FRA diagnosis of transformer faults, *IEEJ Transactions on Power & Energy*, vol. 7, no. 127, pp. 791-796, 2007.

[2] M. Tahir, S. Tenbohlen, FRA lookup charts for the quantitative determination of winding axial displacement fault in power transformers, *IET Electric Power Applications*, vol. 14, no. 12, pp. 2370 – 2377, 2020

[3] V. Nurmanova, M. Bagheri, A. Zollanvari, A new transformer FRA measurement technique to reach smart interpretation for Inter-Disk faults, *IEEE Transactions on Power Delivery*, vol. 34, no. 4, pp. 1508-1519, 2019.

[4] B. Biswas, L. Satish, Analytical expressions to link SCNF and OCNF of transformer windings to their inductances and capacitances for Configurations. *IEEE Transactions on Power Delivery*, vol. 34, no. 4, pp. 1725-1735, 2019.

[5] J. Duan, Y. He, X. Wu, Anti-Interference deep visual identification method for fault localization of transformer using a winding model, *Sensors*, vol. 19, no. 19, 4153, 2019.

[6] A, Abu-Siada, Mohamed, Estimating power transformer high frequency model parameters using frequency response analysis, *IEEE Transactions on Power Delivery*, vol. 35, no. 3, pp. 1267-1277, 2019.

[7] L. J. Zhou, J. F. Jiang, X. Y. Zhou, Z. Y. Wu, T. Lin, D. Y. Wang, Detection of transformer winding faults using FRA and image features, *IET Electric Power Applications*, vol. 14, no. 6, pp. 972–980, 2020.

[8] T. A. Hossein, V. Abolfazl, Effect of the asymmetrical axial displacement of transformer windings on FRA characteristics, *Journal of Critical Reviews*, vol. 7, no. 2, pp. 469-476, 2020.

[9] S. Arumugam, Experimental validation of using frequency response analysis method in measuring inter-winding capacitance of power transformers, *Engineering Reports*, vol. 1, no. 5, e12079, 2019.

[10] A. D. Anurag, H. Noureddine, G.Huw, S. A. Naji, B. Braham, J. Sheshakama, I. Hisatoshi, K. Tadashi, T. Yasuhiko, Winding turn-to-turn short-circuit diagnosis using FRA method: sensitivity of measurement configuration, *IET Science, Measurement & Technology* , vol. 13, no. 1, pp.17-24, 2019.

[11] S. C. Moustafa, M. Samir, H. Hamza, Low and high frequency model of three phase transformer by frequency response analysis measurement, *Open Physics*, vol. 16, no. 1, pp.117-122, 2018.

[12] R. A. Ali, R. M. Mohammad, A. Zakieh, Diagnosis and clustering of power transformer winding fault types by cross-correlation and clustering analysis of FRA results, *IET Generation, Transmission & Distribution*, vol. 12, no. 19, pp.4301-4309, 2018.

[13] M. Pritam, L. Satish, Estimating the equivalent air-cored inductance of transformer winding from measured FRA, *IEEE Transactions on Power Delivery*, vol. 33, no. 4, pp. 1620-1627, 2018.

[14] C. X. Li, T. Y. Zhu, X. Qi, C. G. Yao, Z. Y. Zhao, Influence of untested winding in FRA test for winding diagnosis, *IET Generation, Transmission & Distribution*, vol. 12, no. 8, pp. 1704-1711, 2018.